Heterogeneous & Homogeneous & Bio- & Nano-

CHEMCATCHEM

CATALYSIS

Accepted Article

Title: Reduction of Propanoic Acid over Pd-promoted Supported WOx Catalysts

Authors: James D Kammert, Gordon Brezicki, Naomi Miyake, Eli Stavitski, and Robert Davis

To be cited as: *ChemCatChem* 10.1002/cctc.201901302

Link to VoR: http://dx.doi.org/10.1002/cctc.201901302

A Journal of

ChemPubSoc Europe

WILEY-VCH

www.chemcatchem.org

10.1002/cctc.201901302

Reduction of Propanoic Acid over Pd-promoted Supported WO_x Catalysts

Dr. James D. Kammert[a], Gordon Brezicki[a], Naomi Miyake[a], Dr. Eli Stavitski[b], and Prof. Robert J. Davis[a,]*

a) University of Virginia Department of Chemical Engineering, 102 Engineer's Way, PO Box 400741, Charlottesville, VA 22904-4741, United States

b) National Synchrotron Light Source II, Brookhaven National Lab, Upton, NY 11973, United States

* To whom correspondence should be addressed: rjd4f@virginia.edu

Abstract

Silica-, titania-, and zirconia-supported tungsten oxide catalysts were synthesized by wetness impregnation techniques. When promoted with Pd, these materials catalyzed the reduction of propanoic acid to 1-propanol at 433 K with a selectivity of up to 92% (13.5% conversion) in atmospheric pressure of H_2. Over Pd-promoted WO_x/TiO_2, the observed orders of reaction were 0.2 in H_2 and 0.7 in propanoic acid, and the apparent activation energy was 54 kJ mol^{-1}. In situ X-ray absorption spectroscopy of Pd-promoted WO_x/SiO_2 revealed a slight reduction of the W from +6 to an average oxidation state of about +5 during H_2 treatment above 473 K. In situ infrared spectroscopy indicated the catalyst surface was covered mostly by propanoate species during reaction. For comparison, supported phosphotungstic acid was also evaluated as a catalyst under identical conditions, but the resulting high acidity of the catalyst was deleterious to alcohol selectivity.

Graphical abstract:

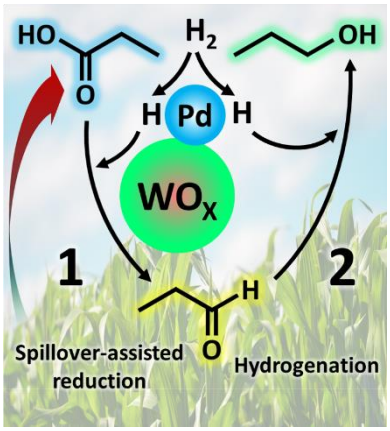

Promoting supported WO_x with Pd results in catalytic activity for the selective (up to 92%) reduction of carboxylic acids to alcohols. Palladium-promoted tungsten oxides were deposited on a variety of supports and characterized using steady-state conversion of propanoic acid, X-ray absorption spectroscopy, and diffuse reflectance infrared Fourier transform spectroscopy.

Keywords: Carboxylic acids, infrared spectroscopy, reduction, tungsten, X-ray absorption spectroscopy

1 Introduction

World demand for oil-derived products, especially chemicals, is expected to grow rapidly in the coming years, as emerging economies develop an increased desire for plastics.[1] While many current technologies still use fossil resources to produce chemicals, a significant effort is underway to develop cost-effective ways to convert biomass to commodity chemicals. Biomass has a similar effective hydrogen-to-carbon ratio as many value-added chemicals, and offers the potential to produce these chemicals at a lower carbon cost in efficient processes.[2] A study performed by the Department of Energy in 2004 found that many of the top building block chemicals that could be produced from biomass are carboxylic acids.[3] Many of these building blocks continue to show promise as potential platform molecules, including short chain carboxylic acids such as lactic acid, succinic acid, 3-hydroxypropanoic acid, and levulinic acid, which can be subsequently upgraded through reduction of their carboxylic acid functionality.[4] As a result, selective reduction of carboxylic acids to produce aldehydes and alcohols is of significant importance to the development of cost-effective technologies for biomass valorization.

Copper-based oxide spinels (such as copper chromite) are well-known catalysts for the reduction of esters (and carboxylic acids) to their corresponding alcohols.[5] Dissociation of the ester into alkoxy and acyl species followed by hydrogenation of the acyl species determined the rate of alcohol formation in this process over copper chromite and supported copper.[6–8] Other works studied the oxides of Re,[9,10] Sn,[11] and Mo[12] promoted by platinum group metals and found they are effective catalysts for the direct catalytic reduction of carboxylic acids. A recent review by Pritchard et al. highlights some of the major recent findings concerning heterogeneous reduction of carboxylic acids.[13] In general, a combination of a reducible metal and an oxophilic metal produces an active catalyst when the two metals are placed in close proximity on a support.

This combination provides adsorbed H atoms to the active site on the metal oxide species, which results in the reduction of the carboxylic acid to an aldehyde intermediate that is subsequently hydrogenated to form the corresponding alcohol. The ability of Pd-promoted supported tungsten oxides, however, to catalyze selective reduction of carboxylic acids to alcohols has not been thoroughly assessed.

Tungsten oxide has a variety of uses as a heterogeneous catalyst, and it is well-known to produce Brønsted acid sites of varying acid strength and site density, depending on the support upon which it is dispersed. Yamaguchi et al. found that WO_x supported on TiO_2, Al_2O_3, and ZrO_2 resulted in the formation of higher densities of acidic sites compared to unsupported WO_x or WO_x supported on SiO_2 and MgO.[14] The resulting acidic sites were catalytically active for 1-butene disproportionation at 373 K. Hino and Arata found that controlled synthesis could produce WO_x/ZrO_2 with superacid properties capable of catalyzing butane isomerization at temperatures as low as 303 K.[15] There is good agreement in the literature that the rate of catalytic isomerization reactions per tungsten atom over WO_x/ZrO_2 is maximized at loadings slightly above the theoretical monolayer coverage of WO_x on the ZrO_2.[16–18] Similar trends in reactivity can be found on supports other than zirconia, where dispersion of the WO_x phase appears to play a critical role.[19] Barton et al. proposed this trend in activity resulted from the formation of reducible polytungstate clusters at optimal intermediate WO_x surface loadings that could stabilize Brønsted acidic protons.[20] Lower loadings of WO_x resulted in irreducible monotungstate species that were less active in the isomerization reactions, while higher loadings resulted in the formation of inactive WO_3 crystallites. The addition of platinum allowed the slight reduction of WO_x polytungstate clusters to occur at mild temperatures (350 K), and resulted in turnover frequencies on the order of 10^2 s^{-1} for *n*-heptane isomerization (473 K, 650 kPa H_2, 100 kPa n-heptane).[21] Characterization

of acidic sites by ex situ and in situ titration with pyridine, ammonia, or sterically hindered pyridine found conflicting trends in Brønsted acid site density with relation to catalytic activity.[17,18,22] Some studies reported a maximum in Brønsted acidity per W atom at intermediate loadings, while others have found that Brønsted acidity per W atom, as well as Lewis acidity per W atom, decreased continuously with increasing W loading. On the other hand, Zr-stabilized, distorted WO_3 crystallites have also been suggested to play a key role in catalysis, for example, in the acid-catalyzed dehydration of methanol to dimethyl ether.[23] Evidently, the nature of catalytically active sites present in supported WO_x catalysts is not completely understood.

Heteropolyanions derived from tungsten, such as phosphotungstic acid ($H_3PW_{12}O_{40}$), also have many uses as heterogeneous acid catalysts.[24] Phosphotungstic acid (PTA) consists of a tetrahedrally coordinated phosphorus atom surrounded by 12 tungsten(VI) oxide octahedra, forming a well-defined Keggin unit (**Figure 1**). The resulting compound can stabilize up to three Brønsted acidic protons, which can be used to catalyze alkylation, condensation, and dehydration reactions, among many other acid-catalyzed reactions. More information about the properties and uses of tungsten heteropolyanions can be found in reviews by Kozhevnikov[24] and Misono.[25] Recent studies have also investigated PTA as a catalyst for conversion of biomass. Examples include the hydrolysis-hydrogenation of cellulose in the presence of Ru/C,[26] and the esterification of triethylene glycol and methacrylic acid.[27]

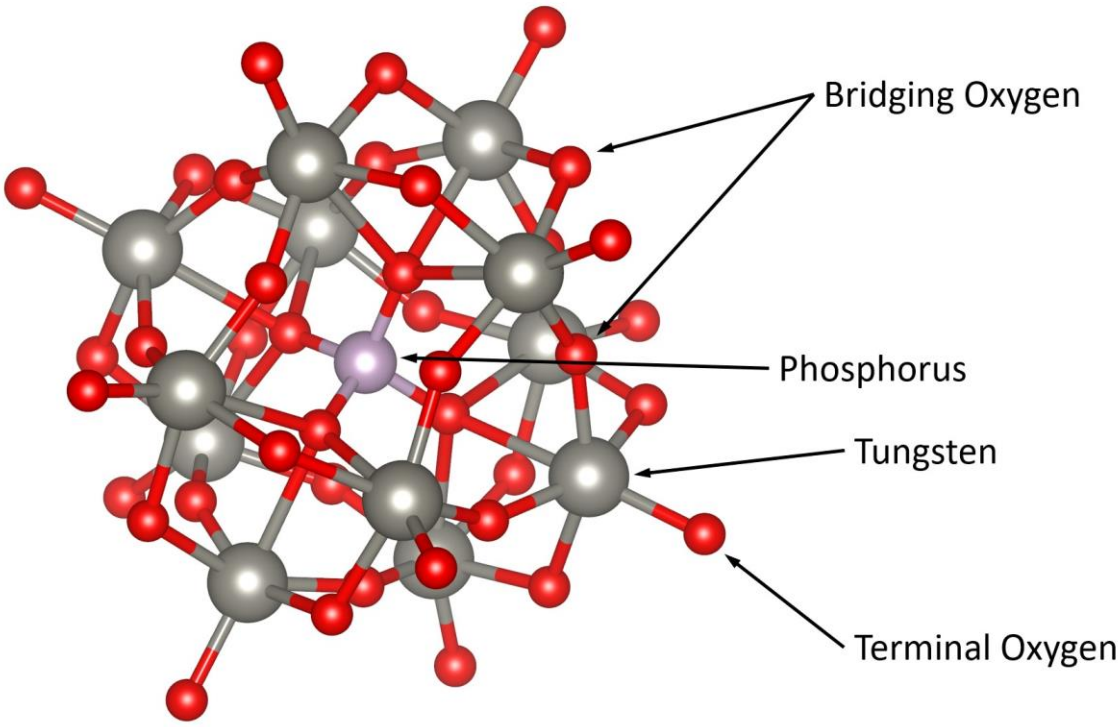

Figure 1: The Keggin structure of phosphotungstic acid, consisting of 12 octahedral tungsten (VI) oxide species surrounding a tetrahedrally coordinated phosphorus atom. The central oxygens connect the central phosphorus atom to the surrounding tungsten octahedra, while bridging oxygens are capable of stabilizing Brønsted-acidic protons.[28]

Few studies have explored tungstates as catalysts for the reduction of carboxylic acids to alcohols. In 1989, tungstate species were identified as a component of the enzymatic reduction of carboxylic acids to aldehydes in *Clostridium thermoaceticum.*[29] Several years later, a patent by Kitson and Williams claimed a mixture of Pt group metals and Re, Mo, and W for the conversion of carboxylic acids to alcohols and esters, but only gave details of the synthesis of several Pd-alloy-promoted Re catalysts.[30] In 1997, Pestman et al. screened a number of metal oxide catalysts for the reduction of acetic acid and reported that WO_3 produced a small amount (17% selectivity) of acetaldehyde in H_2 at 723 K, while the majority product was acetone.[31] In 2013, a patent for a catalyst comprised of tungsten trioxide WO_3, an alkaline earth metal promoter, and a Sn-promoted

transition metal component was claimed by Jevtic et al. for the reduction of carboxylic acids to alcohols.[32] The catalyst could also be promoted by a wide range of transition metals including Pd, but no metal was specifically preferred. Recent studies by Gosselink and Hollak found that bulk WO_3 and W_2C performed hydrodeoxygenation of stearic acid, tristearin, and methyl stearate to C_{17} and C_{18} hydrocarbon products at 523 K, but few oxygenate products were observed under the conditions studied.[33,34] Palladium-promoted WO_x/Al_2O_3 has demonstrated activity for the hydrodeoxygenation of guaiacol,[35] and Pt-promoted WO_x/Al_2O_3 and WO_x/ZrO_2 were active in the hydrogenolysis of glycerol to 1,3-propanediol and could be promoted with SiO_2 addition.[36,37] These previous findings suggest that Pd- and Pt-promoted WO_x materials have the potential to catalyze the selective reduction of carboxylic acids to alcohols.

In this work, we investigated the catalytic activity of SiO_2-, TiO_2-, and ZrO_2-supported Pd-promoted WO_x and compared them to supported phosphotungstic acid (PTA) in the gas-phase reduction of propanoic acid. Biomass conversion processes are often carried out in the liquid phase and are applied to molecules that may sometimes have multiple functional groups (e.g. lactic, succinic, 3-hydroxypropionic, and levulinic acids mentioned earlier). To generate insights specifically about the role of the metal-oxide and metal-support interactions, however, a simplified gas phase system was chosen to study the reduction of a short-chain fatty acid as a surrogate for longer chain free fatty acids that can be produced by fermentation of sugars by engineered microorganisms.[38] The chosen system was expected to be free from complicating effects of solvent interaction with the active site or leaching of the active components (such as phosphotungstic acid, which is soluble in polar media) and did not require extreme H_2 pressures to operate. The adsorption of H_2 and CO was performed to estimate the dispersion of Pd and explore the effect of spillover on H_2 uptake by WO_x. Temperature-programmed reduction and in

situ X-ray absorption spectroscopy were used to follow changes in structure of the WO_x before and after treatment of the catalysts in flowing H_2, which were correlated to catalyst activity. In situ diffuse reflectance infrared Fourier transform spectroscopy provided insights on the species present on the tungsten oxide and support surfaces.

2 Experimental Methods

2.1 Catalyst Synthesis

Silica-supported (Fuji Silysia Chemical Ltd, 511 $m^2 g^{-1}$, 75-150 μm particle size) 8 wt % W (W/SiO_2) and 1 wt % Pd, 8 wt % W (PdW/SiO_2) catalysts were synthesized by the incipient wetness impregnation method. The desired loading of tungsten was introduced as ammonium metatungstate hydrate (Aldrich, 99.99%) to an aqueous solution equal to the pore volume of the SiO_2. The solution was added to the support until the point of incipient wetness. The mixture was dried at 383 K in ambient air, then heated in flowing air to 773 K over 3 h and held at 773 K for 3 h in flowing air. This process was repeated for the desired loading of Pd (using aqueous tetraaminepalladium(II) nitrate, 10 wt%, Aldrich). Titania- and zirconia- supported 8 wt % W (W/TiO_2, W/ZrO_2) and 1 wt % Pd, 8 wt % W (PdW/TiO_2, PdW/ZrO_2) catalysts were synthesized by first adding 5 g of either TiO_2 (Degussa P25, 47 $m^2 g^{-1}$) or $ZrO(OH)_2$ (MEL Chemicals, 420 $m^2 g^{-1}$) to 80 cm^3 of distilled, deionized water (16.8 MΩ), and then dissolving the desired loading of tungsten as ammonium metatungstate hydrate into this suspension. The suspension was dehydrated in a rotary evaporator at 353 K, and then dried at 383 K overnight in ambient air. The dried material was then heated in flowing air to 773 K over 3 hours, held in flowing air at 773 K for 3 h, cooled, and sized to obtain a particle size of between 55 and 180 μm in diameter. The desired loading of Pd was then added as an aqueous solution of tetraaminepalladium(II) nitrate by the incipient wetness procedure outlined above, subjected to the same 773 K treatment in air, and

then re-sized to obtain particles between 55 and 180 μm in diameter. Phosphotungstic acid hydrate (Sigma Aldrich, reagent grade) and Pd-promoted phosphotungstic acid (1 wt % Pd, 8 wt % W) catalysts supported on SiO_2 (PTA/SiO_2 and PdPTA/SiO_2) and TiO_2 (PTA/TiO_2 and PdPTA/TiO_2) were also synthesized using the incipient wetness impregnation method. To avoid decomposition of the phosphotungstic acid (PTA) supported on SiO_2 and TiO_2, Pd was added first by the incipient wetness impregnation procedure for Pd addition described earlier, and then an aqueous solution of PTA was added until the point of incipient wetness to the support. The supported PTA was dried at 383 K in ambient air overnight prior to use.

2.2 Catalytic Reactions

The effects of catalyst pretreatment and reaction conditions on the reduction of propanoic acid (Sigma Aldrich, 99.5%) in H_2 (Praxair, 5.0) and D_2 (Praxair, 2.7) were studied in the gas phase using a packed-bed downward flow reactor. Propanoic acid was supplied from a stainless-steel vapor saturator equipped with a thermocouple to measure the saturator temperature. The reactor consisted of a stainless-steel tube with inner diameter of 0.46 cm, enclosed in a cylindrical aluminum jacket 3.8 cm in diameter, which was heated externally. The reaction temperature was measured by a thermocouple inserted from the top of the reactor tube into the middle of the catalyst bed, which was supported in the center of the reactor tube on a plug of glass wool. Prior to catalytic testing, all lines and saturators leading to the reactor were purged with N_2 for at least 10 min. The reduction of propanoic acid (0-0.5 kPa) was studied between 403 and 433 K, at a total pressure of 0.1 MPa composed of H_2 (0-0.1 MPa) in a balance of N_2. The components in the product stream were separated using an on-line SRI 8610C gas chromatograph (GC) equipped with an MXT-WAX (0.53 mm i.d., 1 μm film thickness, 30 m) column and quantified using a flame-ionization detector (FID).

The fractional conversion (f_i) and product selectivity of propanoic acid (i) to products (j) were obtained using equations (1) and (2):

$$f_i = \frac{\sum M_j}{M_i + \sum M_j} \quad (1)$$

$$S_j = \frac{M_j}{\sum M_j} \quad (2)$$

where M_j is defined as the moles of carbon product j. Hydrocarbon products having carbon numbers below C_6 could not be separated using the MXT-WAX column, and therefore were grouped together as light hydrocarbons, or LHC, for analysis.

2.3 Catalyst Characterization

The chemisorption of H_2 (Praxair, 5.0) and CO (Praxair, 3.0) was performed using a Micromeritics ASAP 2020 instrument. Prior to analysis, each sample was heated to 473 K in flowing H_2 at 10 K min^{-1}, then held at 473 K for 1 h under flowing H_2. The samples were subsequently evacuated at 473 K for 3 h, before cooling to 373 K or 308 K to perform the H_2 or CO chemisorption, respectively. Dihydrogen or carbon monoxide was dosed over the range of 0.13 to 67 kPa. The reported chemisorption values were obtained by extrapolating the probe molecule uptake in the high pressure linear region of the isotherm to zero pressure, which was considered the saturated monolayer coverage.

In situ X-ray absorption spectroscopy (XAS) at the tungsten L_I and L_{III} edges and Pd K edge was carried out on beamline 8-ID of the National Synchrotron Light Source II (NSLS-II) at Brookhaven National Laboratory in Upton, New York, operated at 3.0 GeV and with a typical current of *ca.* 325 mA. All experiments were performed using the Si(111) double crystal monochromator with uncoated Si and Pt-coated higher harmonic rejection mirrors, for W and Pd edges respectively, and a spot size of 0.4 mm. Samples were prepared for analysis by packing the

desired loading of catalyst into a 6 in (0.25 in OD) stainless-steel tube outfitted with Kapton windows and gas tight fittings to allow for sample heating and gas treatment. Samples were held in place in the stainless-steel tubes by supporting the catalyst bed on either side with a plug of shredded graphite felt (AvCarb Felt G200). Prior to treatment, each of the individually fed reactor tubes was flushed with He at 20 $cm^3\ min^{-1}$ for 10 min to remove any residual O_2 in the tubes. Temperature-programmed reduction studied at the W L edges was carried out by initiating the flow of H_2 at 20 $cm^3\ min^{-1}$, waiting for 5 min to allow replacement of the He atmosphere with H_2, and then ramping the temperature at 3 K min^{-1} from ambient temperature to 673 K. Samples were then cooled in He to room temperature. At the Pd K edge, samples were heated at 3 K min^{-1} from ambient temperature to 473 K. After holding the temperature at 473 K for 45 min, the samples were heated to 673 K at 10 K min^{-1}, then cooled to 373 K to collect spectra.

Spectra obtained from X-ray absorption spectroscopy were processed and analyzed using the Demeter software package, written by Bruce Ravel.[39] Prior to analysis, X-ray absorption near-edge structure (XANES) and X-ray absorption fine structure (EXAFS) were background corrected and normalized uniformly at each edge using Athena, an XAS analysis program that is part of the Demeter software package. The oxidation state of the W component of each sample was estimated using the measured position of the W L_I and L_{III} edges. The edge position at the W L_I edge was arbitrarily determined at 0.75 times the normalized absorbance height to minimize interference with the presence of the observed pre-edge feature of the W^{VI} oxide, while the W L_{III}-edge position was arbitrarily determined at a step height of unity in the normalized absorbance spectrum to account for the position of the white line. Local coordination structure and EXAFS were analyzed at the W L_{III} and Pd K edges. Powders of WO_2 (Alfa Aesar, 99.9%), WO_3 (Aldrich, 99.995%), and ammonium metatungstate hydrate were used as standards at the W L_I and L_{III} edges, while Pd foil

(Goodfellow, 12.5 μm, 99.95%) and PdO (Aldrich, 99.999%) were used as standards at the Pd K edge. The WO_3 and Pd foil standards were used as energy references at their respective absorption edges. Powder standards were prepared by grinding each powder thoroughly, mixing with boron nitride (Aldrich, 98%), and then compressing the mixture into a self-supporting wafer using a hydraulic press. The wafers were then affixed to Kapton tape and placed in the beam path for measurement.

In situ infrared spectra of propanoic acid adsorbed on PdW/TiO_2 and W/TiO_2 were obtained using diffuse reflectance infrared Fourier transform spectroscopy (DRIFTS). Spectra were recorded using a Bruker Vertex 70 FTIR spectrometer equipped with a liquid-nitrogen-cooled MCT detector and a Harrick Praying Mantis in situ reactor cell with 5 mm ZnSe windows. Spectra were collected every 20 min, by averaging 800 scans at a resolution of 2 cm^{-1}. The inlet gases were purified using an OMI purifier (Supelco) upstream of a stainless-steel propanoic acid vapor saturator with a bypass line leading to the in situ cell. Prior to data collection, samples were ramped to 473 K in flowing H_2, and then cooled to 413 K in H_2 for analysis. Each sample was exposed to 0.3 kPa of propanoic acid in 0.1 MPa H_2 flowing at 15 cm^3 min^{-1} until the sample reached a steady state (approximately 120 min). The flow was then switched to bypass the in situ cell, thus allowing the cell to be purged with pure H_2. Again, spectra were recorded until the sample reached the new steady state under purging conditions. All resulting spectra were normalized to a reference spectrum taken prior to exposure of the sample to propanoic acid at 413 K in H_2, and converted to Kubelka-Munk units using the Kubelka-Munk equation.[40]

3 Results

3.1 Influence of Catalyst Composition and Pretreatment on Propanoic Acid Reduction

The catalytic reduction of 0.5 kPa propanoic acid in 0.1 MPa H_2 at 433 K was studied over

Pd-promoted W oxide and phosphotungstic acid supported on SiO_2, TiO_2, and ZrO_2. The steady-state rate and product distribution of propanoic acid reduction are shown for each catalyst studied (fresh and after pretreatment in H_2 at 673 K) in **Figure 2**. Tungsten oxide and phosphotungstic acid without a Pd promoter were completely inactive for the conversion of propanoic acid

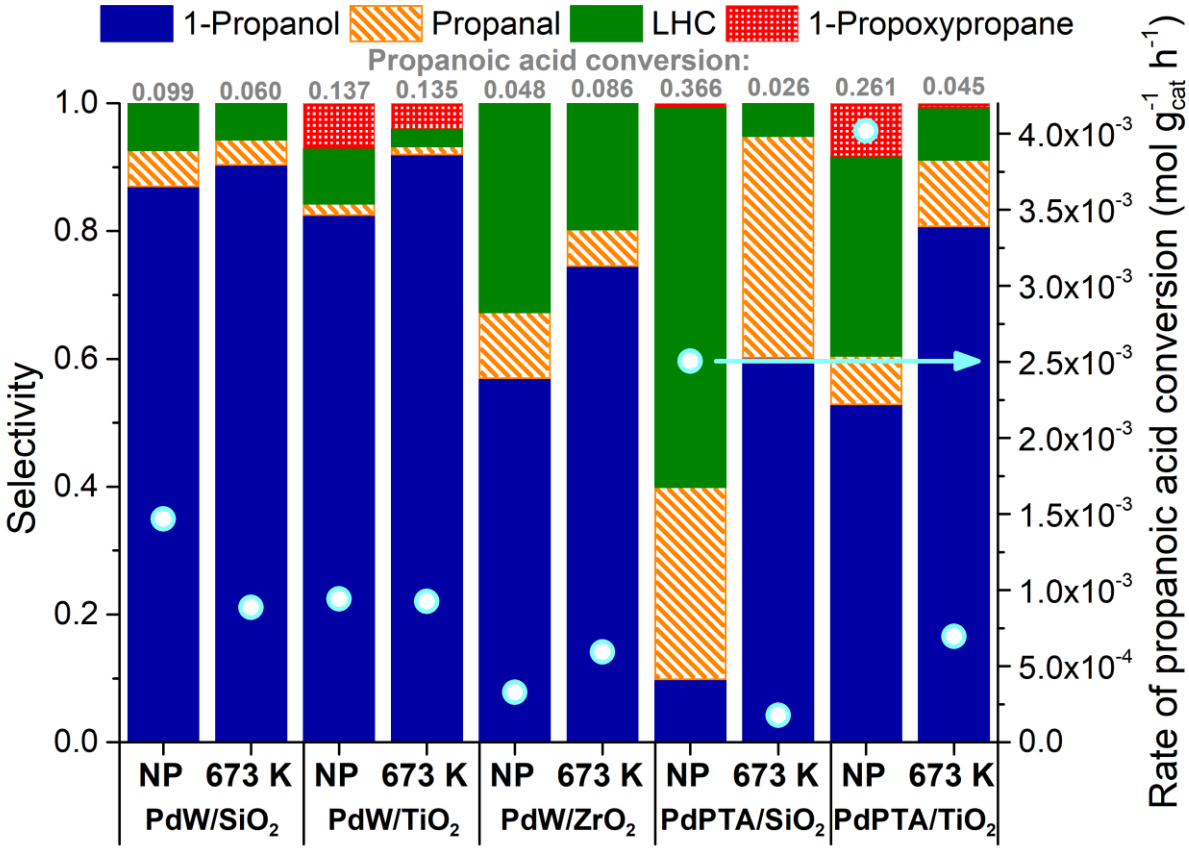

Figure 2: Steady-state rate and product distribution of propanoic acid (0.5 kPa) reduction over SiO_2-, ZrO_2-, and TiO_2-supported Pd-promoted W-based catalysts in 0.1 MPa H_2 at 433 K. Bars correspond to product selectivity on the left axis, while light blue circles correspond to the rate of propanoic acid conversion on the right axis. Values above the bars indicate conversion of acid. NP indicates no in situ H_2 pretreatment, while 673 K indicates a 1 h pretreatment in situ in flowing H_2 at 673 K prior to reaction.

under the conditions studied. Whereas fresh PdW supported on ZrO_2 was active for propanoic acid conversion (PdW/ZrO_2 NP in **Figure 2**), pretreatment of the catalyst for 1 h in H_2 at 673 K nearly doubled the observed the rate of propanoic acid conversion and increased the selectivity towards oxygenated products (propanal and 1-propanol). Fresh PdW/TiO_2 was more active than PdW/ZrO_2, and more selective to oxygenated products, although a small amount of 1-propoxypropane was also formed as a product. **Figure 2** also shows that pretreatment of the PdW/TiO_2 in H_2 at 673 K, compared to a non-pretreated (NP) catalyst, did not have any significant effect on the rate of propanoic acid conversion, but selectivity to light hydrocarbons was reduced by the treatment, leading to a 1-propanol selectivity of 92% at 13.5% conversion of the acid. Fresh SiO_2-supported PdW demonstrated the highest rate of propanoic acid reduction of the supported WO_x catalysts under the conditions studied, and was 87% selective to 1-propanol at 9.9% acid conversion. Pretreatment of the PdW/SiO_2 catalyst in H_2 at 673 K resulted in a loss of nearly half of the activity of the fresh catalyst (**Figure 2**).

Although fresh catalysts prepared with phosphotungstic acid were the most active for propanoic acid conversion, they were 25-50% less selective to 1-propanol (at conversions of 26 to 36%) and produced more light hydrocarbon products. At the conversion levels reported in **Figure 2**, fresh PdPTA/TiO_2 exhibited 5 times higher selectivity to alcohols than PdPTA/SiO_2, while retaining the improved activity of the PTA. On TiO_2-supported catalysts, the formation of 1-propoxypropane was also observed. Formation of ethers has been previously observed using TiO_2-supported W oxide and phosphotungstic acid catalysts.[41,42] As treatment at 673 K is known to decompose PTA,[43] the loss of activity in the PTA catalysts after 673 K treatment in flowing H_2 is not surprising.

3.2 Influence of Reaction Conditions

The rate of reduction of carboxylic acids over fresh PdW/TiO_2 and $PdPTA/TiO_2$ slowly decreased over time, with $PdPTA/TiO_2$ deactivating faster than PdW/TiO_2. The PdW/TiO_2 lost 18% of its activity over 15.75 h time on stream, while the $PdPTA/TiO_2$ lost 40% of its activity over 21.5 h on stream. The rate of propanoic acid reduction versus inverse flowrate is plotted in **Figure 3**(a). Differential conversion that could be used to evaluate a rate was not achieved until conversion was below 5% over $PdPTA/TiO_2$, and below 3% over PdW/TiO_2. The selectivity of propanoic acid conversion towards 1-propanol decreased in favor of propanal as conversion was lowered. This influence of conversion on selectivity is plotted in **Figure 4** and is consistent with a two-step alcohol formation reaction proceeding through an aldehyde intermediate, which has been reported previously.[44] Under differential conditions, the influence of temperature on the rate of reaction was measured and is summarized in **Figure 3**(b). The apparent activation energy for propanoic acid conversion was 54 kJ mol^{-1} over PdW/TiO_2 (**Figure 3**(b)) and the orders of reaction with respect to propanoic acid pressure and H_2 pressure were 0.7 and 0.2, respectively, as determined from the results reported in **Figure 3**(c) and (d). Similar behavior was observed over the $PdPTA/TiO_2$, shown in **Figure S.1** in the supplemental information.

The influence of H_2 pressure on product selectivity is shown in the supplemental information in **Figure S.2**. While changing the H_2 pressure did not have a strong effect on the rate of propanoic acid reduction, lowering the H_2 pressure first leads to an increase in 1-propanol selectivity, followed by decreasing selectivity as the H_2 pressure is lowered further. Moreover, the rate of propanoic acid conversion became immeasurably small when H_2 was completely removed from the reactant stream. An inverse kinetic isotope effect of 0.91 was observed when the H_2 in

10.1002/cctc.201901302

the reactant stream was replaced by D_2 (**Table 1**) during the reduction of propanoic acid by PdW/TiO_2.

10.1002/cctc.201901302

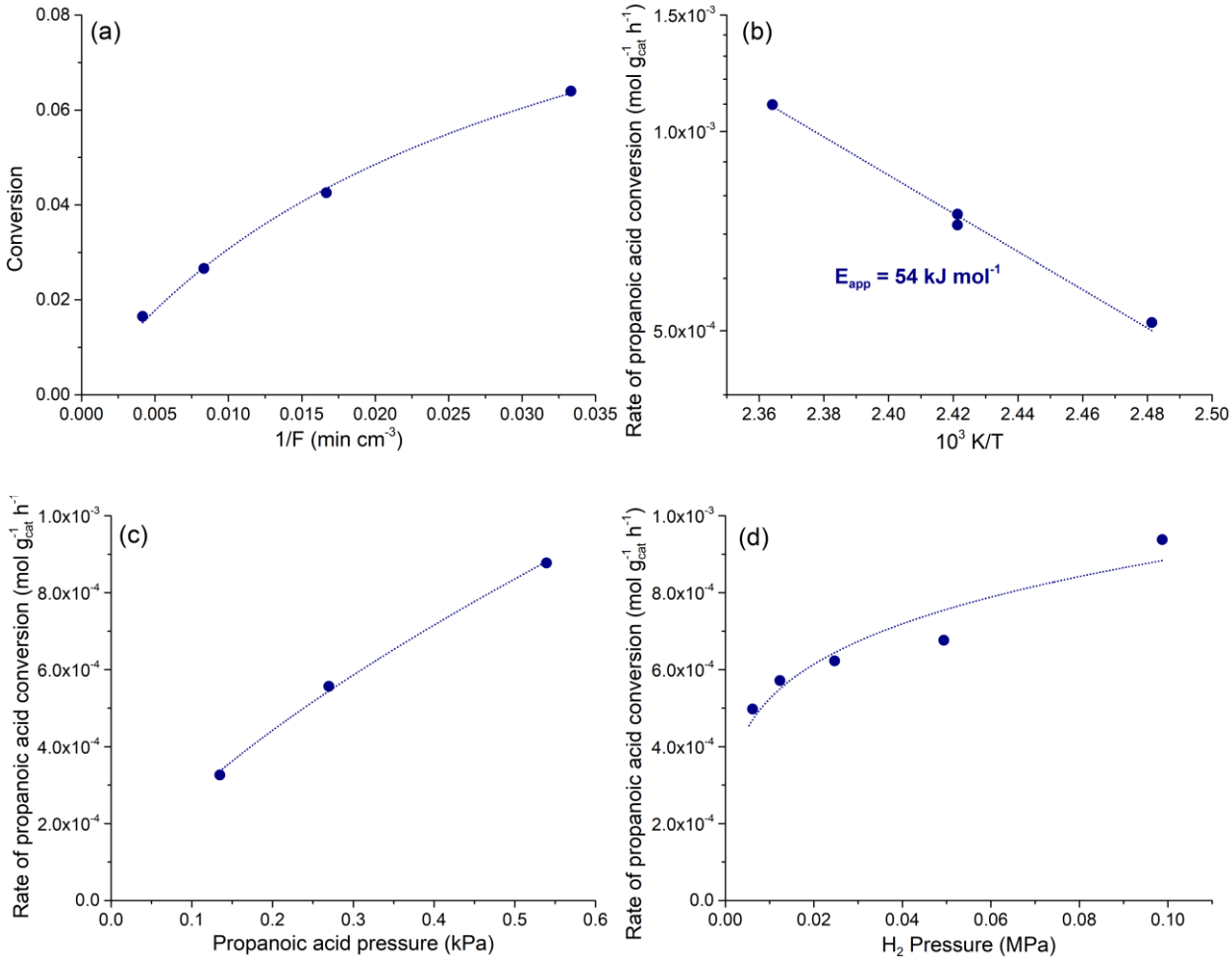

Figure 3: (a) Influence of flow rate on conversion, (b) influence of temperature on rate of propanoic acid conversion, (c) influence of propanoic acid pressure on rate of conversion, and (d) influence of H_2 pressure on rate of conversion during propanoic acid reaction using fresh PdW/TiO_2. All reactions were carried out at 413 K in 0.5 kPa propanoic acid and 0.1 MPa H_2 unless otherwise specified. Dotted lines have been inserted to highlight observed trends.

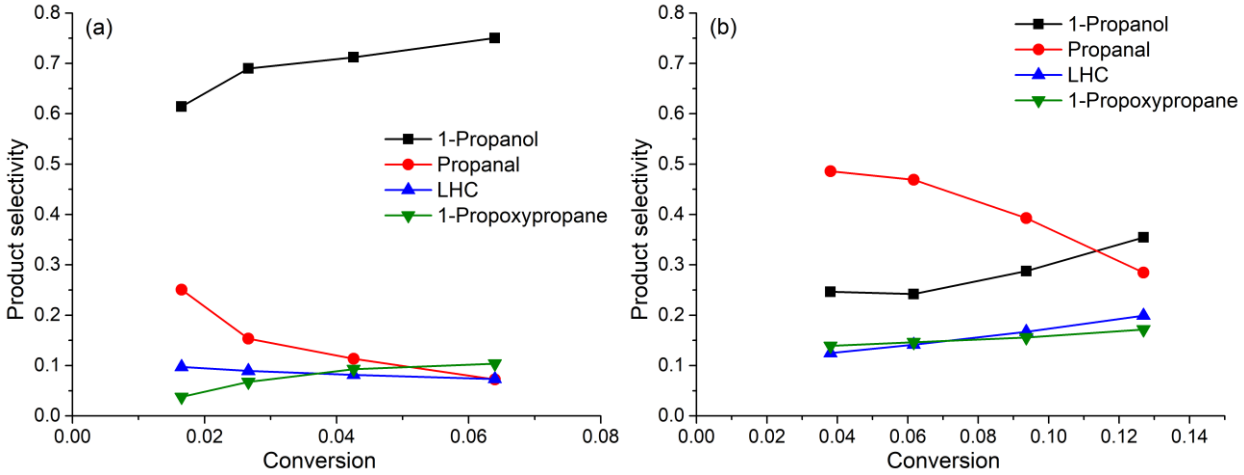

Figure 4: Selectivity versus conversion for the reduction of propanoic acid in 0.5 kPa propanoic acid and 0.1 MPa H_2 at 413 K over (a) PdW/TiO_2 and (b) $PdPTA/TiO_2$. Solid lines are linear interpolation between data points.

Table 1: Comparison of rate of reduction of 0.5 kPa propanoic acid in 0.1 MPa H_2 or D_2 at 413 K over PdW/TiO_2.

Catalyst	H_2/D_2	Conversion	Rate of reduction [mol g_{cat}^{-1} h^{-1}]	Product selectivity				Overall isotope effect ($rate_H/rate_D$)
				1-Propanol	Propanal	LHC	1-Propoxypropane	
PdW/TiO_2	H_2	6.7%	4.5×10^{-4}	0.74	0.07	0.07	0.11	**0.91**
	D_2	7.4%	4.9×10^{-4}	0.74	0.06	0.07	0.12	

3.3 Adsorption of H_2 and CO

The adsorption of H_2 and CO on Pd-promoted WO_x and PTA revealed differences in H_2 uptake by the TiO_2 and SiO_2 supported catalysts (**Table 2**). The calculated Pd dispersions of PdW/TiO_2 and $PdPTA/TiO_2$, assuming a ratio of 1.0 $H/Pd_{surface}$ for TiO_2 supported Pd, were 62% and 58%, respectively. Assuming a ratio of 0.53 $CO/Pd_{surface}$,[45] the calculated Pd dispersions of PdW/TiO_2 and $PdPTA/TiO_2$ were 69% and 71%, respectively. In contrast, the calculated Pd dispersions of PdW/SiO_2 and $PdPTA/SiO_2$, assuming a ratio of 1.0 $H/Pd_{surface}$ for SiO_2 supported Pd, were 36% and 32%, respectively. Assuming a ratio of 0.75 $CO/Pd_{surface}$ for the silica-supported catalysts,[46] the calculated Pd dispersions of PdW/SiO_2 and $PdPTA/SiO_2$ were 25% and 40%, respectively. Regardless of probe molecule, the dispersion of the Pd component is high and corresponds to metal particle sizes ranging from 2 to 4 nm.

Table 2: Total chemisorption uptake of H_2 and CO on Pd-promoted WO_x catalysts.

	Chemisorption [μmol g_{cat}^{-1}]			
Sample	H_2 (373 K)	CO (308 K)	$H/Pd^{[a]}$ (373 K)	$CO/Pd^{[a]}$ (308 K)
PdW/TiO_2	33	39	0.62	0.37
$PdPTA/TiO_2$	31	40	0.58	0.38
PdW/SiO_2	19	20	0.36	0.19
$PdPTA/SiO_2$	17	32	0.32	0.30

(a) Calculated using nominal weight loading of 1 wt % Pd

3.4 X-Ray Absorption Spectroscopy

The X-ray absorption near edge structure (XANES) of PdW/SiO_2 and W/SiO_2 was investigated at the W L_I and L_{III} edges during in situ H_2 temperature programmed reduction (TPR) to determine the role of pretreatment on the electronic structure and coordination environment of the W. As reported earlier, the treatment of PdW/SiO_2 at 673 K in H_2 results in a loss of nearly half of its catalytic activity (**Figure 2**). The W L_I-edge energy of the PdW/SiO_2 and W/SiO_2 samples, measured at a step height of 0.75 in the normalized spectrum, was followed as the samples were

heated in flowing H_2 up to 673 K (**Figure S.5**). On exposure of the samples to H_2, the W L_I-edge energy of the PdW/SiO_2 and W/SiO_2 energy remained fairly constant until 570 K. Above 570 K, the PdW/SiO_2 and W/SiO_2 L_I-edge positions started to shift to lower energies, and continued to shift monotonically until the end of the experiment. As shown in **Figure 5**, the W L_I-edge position of PdW/SiO_2 and W/SiO_2 both shifted 1.2 eV to lower energy over the course of the H_2-TPR experiment. The pre-edge features of both catalysts also shifted to slightly lower energy and increased in intensity during the H_2 treatment, which is consistent with an increased distortion of the octahedral W center in WO_x.[47]

10.1002/cctc.201901302

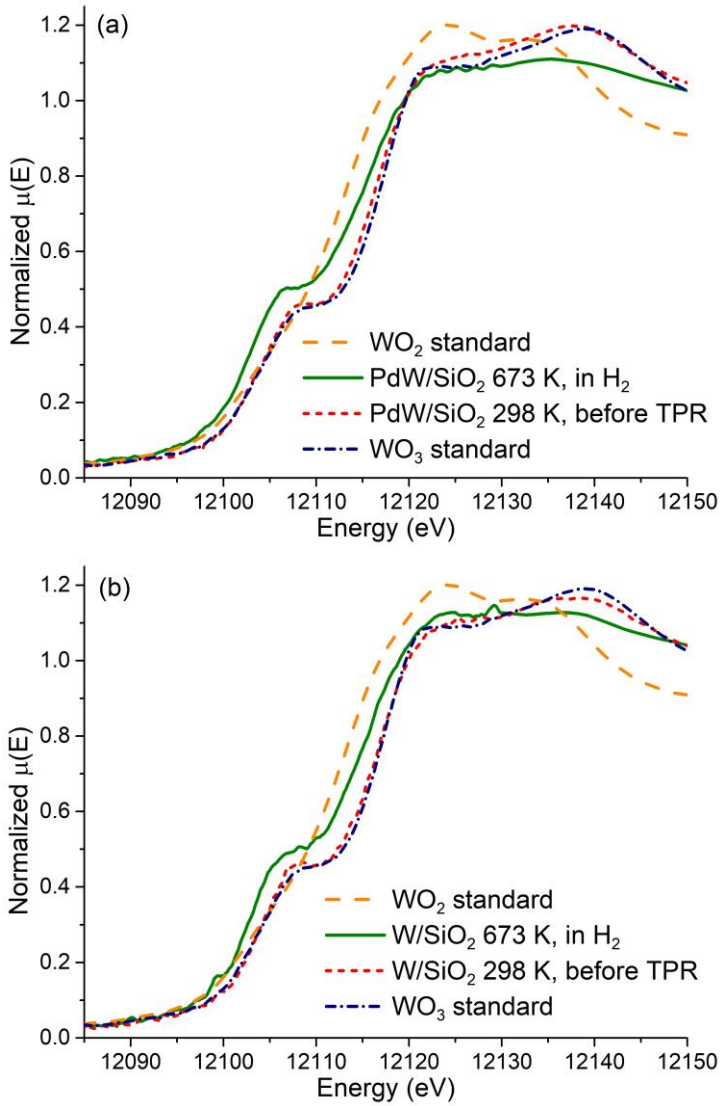

Figure 5: (a) The W LI-edge XANES of PdW/SiO2 before pretreatment (short dash) and at 673 K in 0.1 MPa flowing H2 (solid) compared to the WO2 (long dash) and WO3 (dash-dot) standard spectra. (b) The W LI-edge XANES of W/SiO2 before pretreatment (short dash) and at 673 K in 0.1 MPa flowing H2 (solid) compared to the WO2 (long dash) and WO3 (dash-dot) standard spectra.

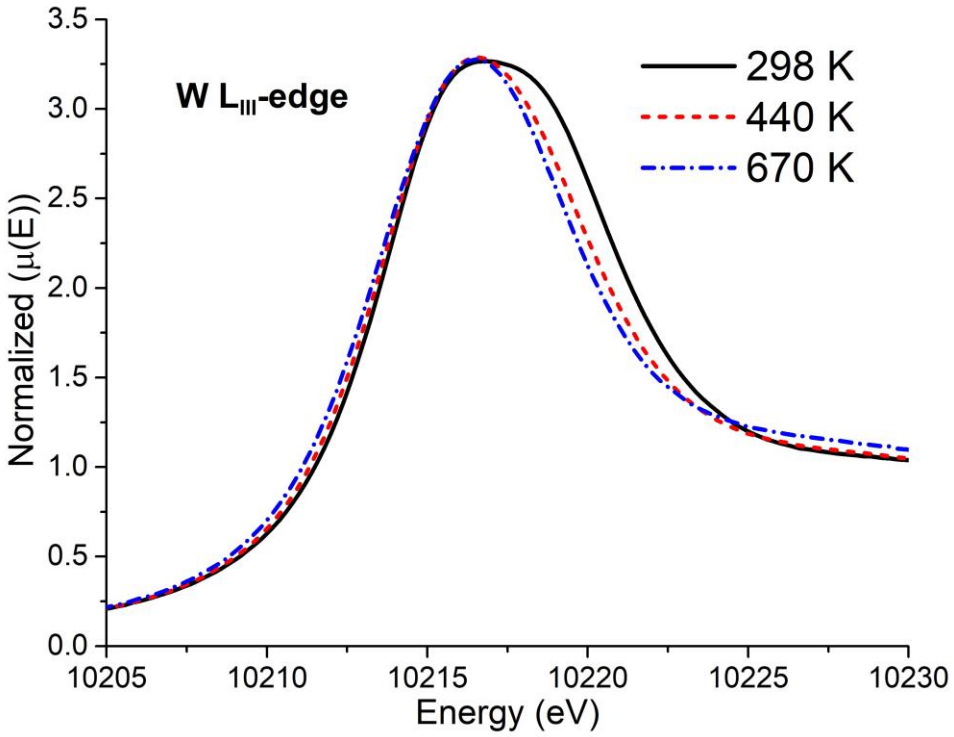

Figure 6: The W L$_{III}$-edge XANES spectra obtained during in situ H$_2$-TPR of PdW/SiO$_2$ in 6% H$_2$/He at 298 K, 440 K, and 670 K.

The W L_{III}-edge XANES were also investigated during H_2-TPR, and representative spectra of PdW/SiO_2 are shown in **Figure 6**. During the H_2-TPR, the whiteline feature was initially asymmetrical, indicative of a slightly distorted octahedral structure typical of clusters of W^{VI}, including ammonium metatungstate and bulk WO_3 (standards are shown in supplemental information **Figure S.6**(a)). Upon heating to 440 K, however, the width of the white line decreased, indicating a decrease in the splitting of the W 5-d orbitals.[47] This behavior has been observed previously in W^{VI} oxides and heteropolyacids, and is attributed to an increase of the distortion of the octahedral coordination geometry of O surrounding W.[47–49] When the temperature was increased from 440 K to 670 K, the W L_{III} edge position also shifted to lower energy, suggesting that W^{VI} was reduced to an average oxidation state between W^{IV} and W^{VI}. Prior to the H_2-TPR, the W L_{III}-edge position of both W/SiO_2 and PdW/SiO_2 was 10205.8 eV. After the

TPR, the edge positions shifted to 10205.2 eV (W/SiO_2) and 10204.9 eV (PdW/SiO_2). The edge positions of the WO_3 and WO_2 standards were 10205.7 and 10204.7 eV, respectively, suggesting that WO_x in both catalysts had been reduced to an average oxidation state between W^{VI} and W^{IV}. Evidently, the Pd-promoted W/SiO_2 was reduced to a lower average oxidation state than the unpromoted W/SiO_2 after the TPR. This reduction behavior is illustrated in the supplemental information (**Figure S.6**(b)), and supports the results obtained at the W L_I edge. Analysis of the W L_{III}-edge EXAFS (shown in **Figure S.7**) from 298 K to 440 K does not indicate any significant change in the coordination number of the first shell W-O scattering path or the W-O scattering path length (**Table S.1**). These results are consistent with minimal reduction of the W (which remained in an oxidation state near W^{VI}) in the PdW/SiO_2 under the conditions studied.

Analysis of the Pd K-edge XANES revealed the as-synthesized catalysts contained only PdO (**Figure S.9**). Qualitative analysis of the Pd K-edge EXAFS prior to reduction found similar Pd-O first shell scattering paths in both samples and the PdO standard. The second shell Pd-Pd scattering paths were less pronounced, however, resulting from a higher dispersion of Pd in the supported PdO particles on the as-synthesized catalysts. Treatment in H_2 at elevated temperature reduced the PdO on both PdW/SiO_2 and $PdPTA/SiO_2$ to metallic Pd (**Figure S.10**). Fitting of the EXAFS resulted in Pd-Pd first-shell coordination numbers of 8.5 and 7.4 in PdW/SiO_2 and $PdPTA/SiO_2$, respectively, after treating the catalysts in H_2 at 673 K. These first-shell coordination numbers (**Table S.2**) are less than the value of 12 expected from bulk Pd, which confirms that Pd in both catalysts was highly dispersed (60-80%), with an approximate particle diameter of between 1 and 2 nm, assuming a spherical particle geometry.[50]

3.5 Diffuse Reflectance Infrared Fourier Transform Spectroscopy

Diffuse reflectance infrared Fourier transform spectroscopy (DRIFTS) was used to probe the surface species present under reaction conditions on the PdW/TiO_2 and W/TiO_2. When propanoic acid in H_2 was introduced to PdW/TiO_2 and W/TiO_2, similar diffuse reflectance spectra were obtained, which are plotted in **Figure 7**. In the C-H stretching region, three weak peaks were visible at 2985, 2949, and 2892 cm^{-1}. These features are shifted to lower wavenumber than the three main visible C-H stretching modes of vapor phase propanoic acid at 2993, 2954, and 2900 cm^{-1}, indicating chemisorption of the propanoic acid on the PdW/TiO_2 surface. A very weak feature in the PdW/TiO_2 spectrum in the presence of propanoic acid was observed at 1965 cm^{-1}, suggesting a small amount of strongly bound CO was present. In the carbonyl stretching region, vibrational modes at 1791, 1772, and 1730 cm^{-1} are consistent with vibrations of vapor phase acid monomers and dimers that have been observed in acetic acid.[51,52] Strong bands at 1661 and 1663 cm^{-1} cm were observed on PdW/TiO_2 and W/TiO_2 respectively, which were not observed during the adsorption of propanoic acid on TiO_2 or Pd/TiO_2. This mode was assigned to an asymmetrical O–C=O vibration characteristic of the binding of propanoic acid to the W component of the catalyst. The broad band at 1511 cm^{-1} is assigned to bridging bidentate adsorption of propanoic acid on TiO_2, while the sharp feature at 1470 cm^{-1} is assigned to a C-H deformation mode in adsorbed propanoic acid.[52] Features at 1435 cm^{-1} and 1418 cm^{-1} are assigned to the symmetrical O–C=O vibrations of bidentate bridging propanoate on TiO_2 and adsorption of propanoate on W, respectively, and the feature at 1380 cm^{-1} is assigned to a C-H bending mode in adsorbed propanoic acid.[52,53] These assignments are summarized in **Table 3**.

When the spectra collected in flowing H_2 after propanoic acid treatment are subtracted from the spectra obtained in flowing H_2 and propanoic acid, the vapor-phase propanoic acid

features are clearly visible (**Figure 7**(a,c)), as is a carbonyl stretching mode near 1680 cm^{-1} (**Figure 7**(b,d)). Carbonyl stretching modes of similar values have previously been reported during acetaldehyde adsorption on Pd/CeO_2[54] and Pt/SiO_2 promoted by Na,[55] and acetic acid reduction on Pt/TiO_2,[56] and were attributed to the formation of acetyl surface species. The difference spectra also revealed a decrease in the intensity of the C-H stretching modes at higher wavenumber than the species observed on both catalyst surfaces in the in situ or H_2 purging spectra, indicating the desorption of more weakly bound propanoic acid species during H_2 purging.

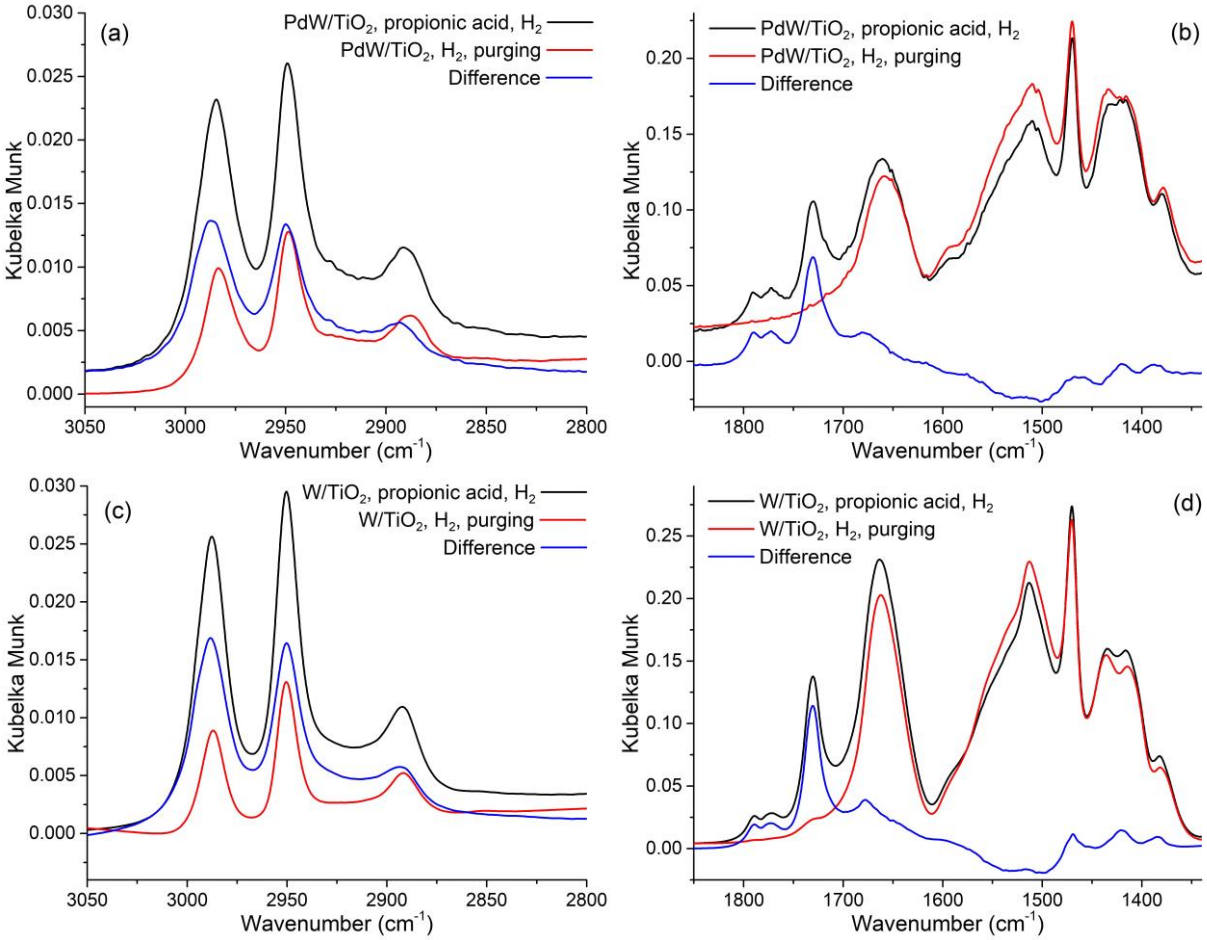

Figure 7: Infrared spectra recorded at a sample temperature of 413 K showing PdW/TiO_2 and W/TiO_2 in the (a, c, respectively) C-H stretching region and (b, d, respectively) carbonyl and backbone deformation region during treatment in 0.3 kPa propanoic acid in 0.1 MPa H_2 and

10.1002/cctc.201901302

after treatment in 0.1 MPa H_2 (purging). Difference spectra were obtained by subtracting the spectra taken during H_2 purging from the spectra obtained during propanoic acid treatment.

Table 3: Assignment of vibrational modes observed during reduction of 0.3 kPa propanoic acid in 0.1 MPa H_2 at 413 K over PdW/TiO_2 and W/TiO_2.

Adsorbent	Conditions	Vibrational mode	Frequency [cm^{-1}]	Assignment
PdW/TiO_2 or W/TiO_2	0.3 kPa propanoic acid, 0.1 MPa H_2, 413 K	ν(OH)	3500-3100 broad	Propanoic acid, water (physisorbed)
		$\nu_a(CH_3)$	2985	Propanoic acid, bidentate[56,57]
		$\nu_a(CH_2)$	2949	Propanoic acid, bidentate
		$\nu_s(CH_3)$	2930-2900 w	Propanoic acid, bidentate
		$\nu_s(CH_2)$	2892	Propanoic acid, bidentate
		ν(C=O)	1791,1772,1732	Propanoic acid, (vapor, monomer and dimer)
			1680	Propanoyl[54–56]
			1661	Propanoic acid, WO_x
		ν_a(O—C=O)	1520	Propanoic acid, bidentate[53,57], TiO_2
		δ(C—H)	1470	Propanoic acid
		ν_s(O—C=O)	1436, 1418	Propanoic acid[53]
		δ(C—H)	1380	Propanoic acid

4 Discussion

4.1 Catalytic Activity of Pd-promoted WO_x and PTA

Promotion of SiO_2-, TiO_2-, and ZrO_2-supported WO_x and PTA with Pd produced active catalysts for the conversion of carboxylic acids that reduced propanoic acid at a higher rate per mass of catalyst than Pd-promoted Re catalysts previously studied under similar conditions. For example, Pd-promoted WO_x (8 wt% W) and Pd-promoted ReO_x (8 wt% Re) supported on the same SiO_2 exhibited a rate of propanoic acid conversion of $1.5 \cdot 10^{-3}$ and $3.0 \cdot 10^{-4}$ mol g_{cat}^{-1} h^{-1}, respectively, at 433 K, 0.5 kPa acid and 0.1 MPa H_2.[58] Prior work found that carboxylic acid reduction is catalyzed by Pt/TiO_2 at the Pt-TiO_2 interface, wherein Pt was believed to supply H to active sites on the TiO_2 surface in a bifunctional surface reaction mechanism.[56,59] More recent studies of carboxylic acid reduction catalyzed by Re and Pd-promoted Re (which are much more active than the Pt/TiO_2 system) have struggled to demonstrate that the cooperation of metal and metal oxide sites is still required to produce a catalytically active site.[44,60–63] Studies suggest that "intimate contact" between Pd and Re must be achieved to produce an active catalyst,[64] but as Re is often reduced to a mixture of oxidized and metallic species under reaction conditions, the active state of the Re is obscured. In this study, the combination of metallic Pd and W oxide produces an active catalyst for carboxylic acid reduction when the two components are placed on the same support. This result suggests that a bifunctional mechanism utilizing a metal (here Pd) to dissociate H_2, which makes adsorbed H species available to the catalytic active site (likely via H spillover) for carboxylic acid reduction on the metal oxide (here WO_x), is responsible for the observed activity , as has been previously proposed in the Pd-promoted Re system.[58]

The observed activity depended strongly on both support and pretreatment of the catalyst, which are believed to have a significant effect on the type, strength, and quantity of acid sites

present on the WO_x surface. Supports such as TiO_2 and ZrO_2, which form Brønsted acid sites when loaded with dispersed WO_x species,[14,17,18] produced catalysts that were not as active for the reduction of propanoic acid as fresh SiO_2-supported WO_x. When Pd-promoted PTA was supported on SiO_2 and TiO_2, higher activity for the reduction of propanoic acid was observed relative to Pd-promoted WO_x on SiO_2 or TiO_2. Despite their higher activity, PdPTA catalysts were only half as selective for the formation of oxygenated products, and the observed rate of formation of oxygenated products over PdPTA was still comparable to the rate of oxygenate formation observed over the PdW catalysts on SiO_2 and TiO_2. In light of this observation, we propose that higher surface densities of Brønsted acid sites are detrimental and lead to less selective reduction of the carboxylic acid functionality, as observed for PdW supported on ZrO_2 and the supported heteropolyacids. Presumably, Brønsted acid sites catalyze unselective dehydration steps that lead to hydrocarbons and ethers. Yamaguchi et al. studied the isomerization of cyclopropane over similarly made WO_x catalysts and found that WO_x/ZrO_2 was more active for the isomerization reaction, while WO_x/TiO_2 was less active and WO_x/SiO_2 demonstrated no activity. This trend followed the previously reported acid site strength of each catalyst, where WO_x/ZrO_2 and WO_x/TiO_2 are claimed to have stronger acid sites, and WO_x/SiO_2 had weaker acid sites.[14] However, the trend in reactivity observed here was the opposite. Apparently, supports that are expected to generate weaker Brønsted acid sites when combined with WO_x can be correlated with higher activity for the reduction of carboxylic acids.

Strong Lewis acid sites may also catalyze the C-O bond breaking of weakly adsorbed carboxylic acids. A positive reaction order in propanoic acid was observed, which contrasted previously studied Re and Pd-promoted Re systems wherein the rate was nearly zero order in acid.[44,58,61] Under similar conditions, Pd-promoted Re was found to reside in an average oxidation

state of Re^{IV}, while the Pd-promoted W studied here was in an average oxidation state between W^{IV} and W^{VI}. A lower density of exposed metallic centers (Lewis acid sites) on W compared to Re might result in fewer adjacent Lewis acidic sites, and weaker interaction between the propanoic acid and the catalyst surface, especially in the absence of bidentate binding of propanoate to the active site.

The weak dependence of the propanoic acid reduction rate on H_2 pressure and lack of a strong kinetic isotope effect are consistent with rate-determining C-O bond breaking of the weakly adsorbed carboxylic acid species in the absence of high coverage of carboxylate species on the active site. These orders of reaction contrast near first-order dependence of reduction rate on H_2 and near zero-order dependence of reduction rate on carboxylic acid concentration observed during carboxylic acid reduction catalyzed by previously studied systems such as Re and Pd-promoted Re.[44,58,61] The observed order in H_2 suggests H availability at the active site in these Pd-promoted WO_x catalysts is not changing significantly (and may be saturated) under the conditions studied. The role of different types of acid sites (Brønsted vs. Lewis), acid site strengths, and acid site quantities in the formation of surface species leading to reduction products merits more detailed investigation.

4.2 Characterization of SiO_2- and TiO_2-supported W

Results from the W L_I-edge and L_{III}-edge XANES suggest that treatment at increased temperature in H_2 results in a slight shift of edge energies to lower values and an increase in intensity of the pre-edge feature at the W L_I edge, consistent with octahedral WO_x species becoming more distorted during H_2 treatment. The energy shifts in the W L_I- and L_{III}-edge XANES indicate that WO_3 PdW/SiO_2 and W/SiO_2 is reduced from W^{VI} to an average oxidation state of between W^{VI} and W^{IV} during H_2 treatment at 673 K. The formation of W bronze by reaction of

WO_3 with H_2 to form H_xWO_3 is well-documented and has potential catalytic applications.[65,66] The formation of a hydrogen bronze on our supported WO_x catalysts may explain the observed changes in the W L_I- and L_{III}-edge spectra (i.e. the shift in the X-ray absorption edge energy of W and increased distortion of the WO_x octahedra) accompanied by an insignificant change in the first shell W-O coordination number and distance as determined by W L_{III}-edge EXAFS analysis. Reactivity results indicate, however, that PdW/SiO_2 loses almost half of its initial activity after pretreatment in H_2 at 673 K. Therefore, reduction of WO_3 to a WO_x of $2<x<3$ phase (perhaps by WO_3 bronze formation) or the disappearance of the monoclinic WO_3 phase may be related to catalyst deactivation.

The most abundant observable species on the surface of the PdW/TiO_2 and W/TiO_2 under reaction conditions was identified as propanoate bound to the WO_x and TiO_2 surfaces, giving characteristic asymmetrical O–C=O vibrational modes in DRIFTS near 1660 cm^{-1} and 1510 cm^{-1}, respectively. The symmetrical O–C=O modes were observed at 1430 cm^{-1} and 1418 cm^{-1}. The splitting between the asymmetrical and symmetrical modes can give insight into the type of interaction between the acid and the surface.[57] A splitting of 80 cm^{-1} between the symmetrical and asymmetrical C–O=O modes is in the range of bidentate and bidentate bridging species. These species have been observed on TiO_2 in the absence of any active metal, and calculated binding modes of acetic acid adsorption on TiO_2 suggest that this species is a bidentate bridging species.[67] In contrast, a splitting of 230 cm^{-1} between the two modes observed in the presence of WO_x is closer to the expected values found in unidentate or asymmetrical bidentate carboxylate species, indicative of weaker binding of the propanoate species on WO_x.[57]

Upon removal of the carboxylic acid from the gas phase over both catalysts, the difference spectra revealed a peak near 1680 cm^{-1}. Peaks in this location have been observed in the past during

acetaldehyde adsorption on Pd/CeO_2,[54] Pt/SiO_2 promoted by Na,[55] and acetic acid reduction over Pt/TiO_2,[56] and were assigned to the formation of acetyl species on the catalyst surface. While this peak is present on both PdW/TiO_2 and W/TiO_2, only PdW/TiO_2 was active for propanoic acid conversion. We propose that this species is a propanoyl intermediate bound to the WO_x surface. Reversible adsorption of the carboxylic acid on WO_x can explain both the observed order of reaction in propanoic acid and the carbonyl stretching modes observed by DRIFTS. Previous computational work suggests metallic surfaces of Pd and Re will be highly covered in strongly bound carboxylate species under reaction conditions.[68] However, the previous computational work suggests that these carboxylate species act as spectators, and weakly bound carboxylic acids are more likely to take part in the reduction reaction. Monodentate adsorption of propanoic acid as observed in DRIFTS and a nearly first order dependence of rate on propanoic acid suggest that the propanoic acid is interacting weakly with the WO_x active site, potentially leading to a higher coverage of reactive intermediates. The observation of propanoyl species suggests the carboxylic acid might proceed through a propanoyl intermediate reversibly bound to WO_x. In the presence of Pt (or Pd), water, and H_2, the transport of reducing H across WO_x to form the H_xWO_3 bronze occurs readily,[69] and is proposed to hydrogenate these propanoyl species to propanal which can be subsequently hydrogenated to 1-propanol on Pd. In the absence of metal function such as Pd, however, it is unlikely that the hydrogenation steps could occur under such mild conditions, resulting in a catalytic "dead end" for the propanoyl surface species along this reaction path.

5 Conclusions

Palladium-promoted SiO_2-, TiO_2-, and ZrO_2-supported WO_x and PTA synthesized by wetness impregnation of ammonium metatungstate and phosphotungstic acid catalyzed the reduction of gas-phase propanoic acid in atmospheric pressure of H_2. Major products of the

reduction included 1-propanol, propanal, 1-propoxypropane, and light hydrocarbons. Treatment of these catalysts at 673 K in flowing H_2 decreased the conversion rates for SiO_2-supported WO_x and SiO_2- or TiO_2-supported PTA relative to untreated samples, whereas the rate over WO_x/TiO_2 remained about the same and the rate over WO_x/ZrO_2 nearly doubled after treatment in H_2 at 673 K. Propanoic acid reduction catalyzed by Pd-promoted WO_x or PTA was 0.2 order in H_2, and 0.7 order in propanoic acid, and a small inverse kinetic isotope of $rate_H/rate_D = 0.91$ during reduction of propanoic acid with D_2 was observed. The 0.2 order in H_2 suggested availability of H to the catalytic active site is nearly saturated under the conditions studied. In contrast, the 0.7 order in propanoic acid and observation of monodentate propanoic acid species in DRIFTS suggested reversible adsorption of the acid to the active site. Adsorption of H_2 and CO suggested higher dispersion of the Pd on the TiO_2 supported catalysts than on the SiO_2 supported catalysts, but the observed rate of carboxylic acid reduction was not directly correlated to Pd dispersion. Instead, Pd is proposed to be responsible for dissociating H_2, making adsorbed H species available to active sites on the WO_x performing carboxylic acid reduction. X-Ray absorption spectra at the W L_I edge indicated that H_2 treatment resulted in the slight reduction of WO_x near reaction temperatures at 440 K and further reduction during 673 K H_2 treatment. Infrared studies of W/TiO_2 and PdW/TiO_2 indicated that the catalyst surface is highly covered in propanoate species, but also contained a small fraction of an unknown carbonyl stretching mode that was assigned to a propanoyl species, suggesting a surface acyl species is formed during reduction of the carboxylic acid on WO_x. The findings reported here offer insight into tungsten-oxide-catalyzed reduction of carboxylic acids to primary alcohols, which has not been reported on previously, and the relevance of surface acid sites to carboxylic acid reduction.

Acknowledgements

This work used beamline 8-ID of the National Synchrotron Light Source II, a U.S. Department of Energy (DOE) Office of Science User Facility operated for the DOE Office of Science by Brookhaven National Laboratory under Contract No. DE-SC0012704. This material is based upon work supported by the National Science Foundation (NSF) under Award No. EEC-0813570. Any opinions, findings, and conclusions or recommendations expressed in this material are those of the author(s) and do not necessarily reflect the views of the NSF. This material is also based upon work partially supported by the U.S. Department of Energy, Office of Science, Office of Basic Energy Sciences, Chemical Sciences, Geosciences, & Biosciences Division under Award Number DE-FG02-95ER14549. GB acknowledges financial support from MAXNET Energy and the University of Virginia.

References

[1] International Energy Agency, *The Future of Petrochemicals*, **2018**.

[2] P. N. R. Vennestrøm, C. M. Osmundsen, C. H. Christensen, E. Taarning, *Angew. Chemie - Int. Ed.* **2011**, *50*, 10502–10509.

[3] T. Werpy, G. Peterson, *Top Value Added Chemicals from Biomass Volume 1 -- Results of Screening for Potential Candidates from Sugars and Synthesis Gas*, **2004**.

[4] J. J. Bozell, G. R. Petersen, *Green Chem.* **2010**, *12*, 539–554.

[5] H. Adkins, R. Connor, *J. Am. Chem. Soc.* **1931**, *53*, 1091–1095.

[6] T. Y. Yan, L. F. Albright, L. C. Case, *Ind. Eng. Chem. Prod. Res. Dev.* **1965**, *4*, 101–107.

[7] J. W. Evans, M. S. Wainwright, N. W. Cant, D. L. Trimm, *J. Catal.* **1984**, *88*, 203–213.

[8] M. A. N. Santiago, M. A. Sánchez-Castillo, R. D. Cortright, J. A. Dumesic, *J. Catal.* **2000**, *193*, 16–28.

[9] H. S. Broadbent, *Ann. N. Y. Acad. Sci.* **1967**, *145*, 58–71.

[10] B. Trivedi, D. Grote, T. Mason, *J. Am. Oil Chem. Soc.* **1981**, *58*, 17–20.

[11] K. Tahara, E. Nagahara, Y. Itoi, S. Nishiyama, S. Tsuruya, M. Masai, *J. Mol. Catal. A Chem.* **1996**, *110*, L5–L6.

[12] L. Chen, Y. Zhu, H. Zheng, C. Zhang, Y. Li, *Appl. Catal. A Gen.* **2012**, *411–412*, 95–104.

[13] J. Pritchard, G. A. Filonenko, R. van Putten, E. J. M. Hensen, E. A. Pidko, *Chem. Soc. Rev.* **2015**, *44*, 3808–3833.

[14] T. Yamaguchi, Y. Tanaka, K. Tanabe, *J. Catal.* **1980**, *65*, 442–447.

[15] M. Hino, K. Arata, *Chem. Lett.* **1988**, *18*, 971–972.

[16] D. G. Barton, S. L. Soled, E. Iglesia, *Top. Catal.* **2006**, *6*, 87–99.

[17] C. D. Baertsch, S. L. Soled, E. Iglesia, *J. Phys. Chem. B* **2001**, *105*, 1320–1330.

[18] N. Soultanidis, W. Zhou, A. C. Psarras, A. J. Gonzalez, E. F. Iliopoulou, C. J. Kiely, I. E. Wachs, M. S. Wong, *J. Am. Chem. Soc.* **2010**, *132*, 13462–13471.

[19] J. E. Herrera, J. H. Kwak, J. Z. Hu, Y. Wang, C. H. F. Peden, J. Macht, E. Iglesia, *J. Catal.* **2006**, *239*, 200–211.

[20] D. G. Barton, M. Shtein, R. D. Wilson, S. L. Soled, E. Iglesia, *J. Phys. Chem. B* **1999**, *103*, 630–640.

[21] E. Iglesia, D. G. Barton, S. L. Soled, S. Miseo, J. E. Baumgartner, W. E. Gates, G. A. Fuentes, G. D. Meitzner, in *Stud. Surf. Sci. Catal.*, **1996**, pp. 533–542.

[22] C. D. Baertsch, K. T. Komala, Y. H. Chua, E. Iglesia, *J. Catal.* **2002**, *205*, 44–57.

[23] E. I. Ross-Medgaarden, W. V. Knowles, T. Kim, M. S. Wong, W. Zhou, C. J. Kiely, I. E. Wachs, *J. Catal.* **2008**, *256*, 108–125.

[24] I. V. Kozhevnikov, *Catal. Rev.* **1995**, *37*, 311–352.

[25] M. Misono, *Catal. Rev.* **1987**, *29*, 269–321.

[26] R. Palkovits, K. Tajvidi, A. M. Ruppert, J. Procelewska, *Chem. Commun.* **2011**, *47*, 576–578.

[27] S. Shanmugam, B. Viswanathan, T. K. Varadarajan, *J. Mol. Catal. A Chem.* **2004**, *223*, 143–147.

[28] B. B. Bardin, R. J. Davis, *Appl. Catal. A Gen.* **2000**, *200*, 219–231.

[29] H. White, G. Strobl, R. Feicht, H. Simon, *Eur. J. Biochem.* **1989**, *184*, 89–96.

[30] M. Kitson, P. S. Williams, *Platinum Group Metal Alloy Catalysts for Hydrogenation of Carboxylic Acids and Their Anhydrides to Alcohols and/or Esters*, **1992**, US5149680A.

[31] R. Pestman, R. Koster, J. Pieterse, V. Ponec, *J. Catal.* **1997**, *168*, 255–264.

[32] R. Jevtic, V. Johnston, H. Weiner, Z. Zhou, *PROCESSES FOR HYDROGENATING*

ALKANOIC ACDS USING CATALYST COMPRISING TUNGSTEN, **2013**, US8536382B2.

[33] R. W. Gosselink, D. R. Stellwagen, J. H. Bitter, *Angew. Chemie - Int. Ed.* **2013**, *52*, 5089–5092.

[34] S. A. W. Hollak, R. W. Gosselink, D. S. van Es, J. H. Bitter, *ACS Catal.* **2013**, *3*, 2837–2844.

[35] U. G. Hong, J. K. Kim, J. Lee, J. K. Lee, J. H. Song, J. Yi, I. K. Song, *Appl. Catal. A Gen.* **2014**, *469*, 466–471.

[36] S. Zhu, X. Gao, Y. Zhu, Y. Li, *J. Mol. Catal. A Chem.* **2015**, *398*, 391–398.

[37] S. Zhu, X. Gao, Y. Zhu, J. Cui, H. Zheng, Y. Li, *Appl. Catal. B Environ.* **2014**, *158–159*, 391–399.

[38] H. Wu, M. Karanjikar, K.-Y. San, *Metab. Eng.* **2014**, *25*, 82–91.

[39] B. Ravel, M. Newville, *J. Synchrotron Radiat.* **2005**, *12*, 537–541.

[40] J. H. Nobbs, *Rev. Prog. Color. Relat. Top.* **1985**, *15*, 66–75.

[41] A. Yada, T. Murayama, J. Hirata, T. Nakashima, M. Tamura, Y. Kon, W. Ueda, *Chem. Lett.* **2018**, *47*, 2017–2019.

[42] K. T. Venkateswara Rao, P. S. N. Rao, P. S. Sai Prasad, N. Lingaiah, *Catal. Commun.* **2009**, *10*, 1394–1397.

[43] G. A. Tsigdinos, in *Top. Curr. Chem.*, Springer-Verlag, Berlin/Heidelberg, **1978**, pp. 1–64.

[44] B. Rozmysłowicz, A. Kirilin, A. Aho, H. Manyar, C. Hardacre, J. Wärnå, T. Salmi, D. Y. Murzin, *J. Catal.* **2015**, *328*, 197–207.

[45] S. J. Tauster, S. C. Fung, R. L. Garten, *J. Am. Chem. Soc.* **1978**, *100*, 170–175.

[46] C. L. M. Joyal, J. B. Butt, *J. Chem. Soc. Faraday Trans. 1* **1987**, *83*, 2757–2764.

[47] S. Yamazoe, Y. Hitomi, T. Shishido, T. Tanaka, *J. Phys. Chem. C* **2008**, *112*, 6869–6879.

[48] F. Hilbrig, H. E. Göbel, H. Knözinger, H. Schmelz, B. Lengeler, *J. Phys. Chem.* **1991**, *95*, 6973–6978.

[49] J. A. Horsley, I. E. Wachs, J. M. Brown, G. H. Via, F. D. Hardcastle, *J. Phys. Chem.* **1987**, *91*, 4014–4020.

[50] A. Jentys, *Phys. Chem. Chem. Phys.* **1999**, *1*, 4059–4063.

[51] J. Bournay, Y. Marechal, *J. Chem. Phys.* **1973**, *59*, 5077–5087.

[52] R. P. Young, *Can. J. Chem.* **1969**, *47*, 2237–2247.

[53] S. R. Tong, L. Y. Wu, M. F. Ge, W. G. Wang, Z. F. Pu, *Atmos. Chem. Phys.* **2010**, *10*, 7561–7574.

[54] H. Idriss, C. Diagne, J. P. Hindermann, A. Kiennemann, M. A. Barteau, *J. Catal.* **1995**, *155*, 219–237.

[55] S. Boujana, D. Demri, J. Cressely, A. Kiennemann, J. P. Hindermann, *Catal. Letters* **1991**, *7*, 359–366.

[56] W. Rachmady, M. A. Vannice, *J. Catal.* **2002**, *207*, 317–330.

[57] K. Nakamoto, in *Infrared Raman Spectra Inorg. Coord. Compd.*, John Wiley & Sons, Inc., Hoboken, NJ, USA, **1987**.

[58] J. D. Kammert, J. Xie, I. J. Godfrey, R. R. Unocic, E. Stavitski, K. Attenkofer, G. Sankar, R. J. Davis, *ACS Sustain. Chem. Eng.* **2018**, *6*, 12353–12366.

[59] W. Rachmady, M. Vannice, *J. Catal.* **2000**, *192*, 322–334.

[60] Y. Takeda, Y. Nakagawa, K. Tomishige, *Catal. Sci. Technol.* **2012**, *2*, 2221.

[61] Y. Takeda, M. Tamura, Y. Nakagawa, K. Okumura, K. Tomishige, *ACS Catal.* **2015**, *5*,

7034–7047.

[62] D. P. Minh, M. Besson, C. Pinel, P. Fuertes, C. Petitjean, *Top. Catal.* **2010**, *53*, 1270–1273.

[63] J. Sá, C. Kartusch, M. Makosch, C. Paun, J. a van Bokhoven, E. Kleymenov, J. Szlachetko, M. Nachtegaal, H. G. Manyar, C. Hardacre, *Chem. Commun. (Camb).* **2011**, *47*, 6590–2.

[64] B. K. Ly, D. P. Minh, C. Pinel, M. Besson, B. Tapin, F. Epron, C. Especel, *Top. Catal.* **2012**, *55*, 466–473.

[65] R. B. Levy, M. Boudart, *Science*, **1973**, *181*, 547–549.

[66] P. G. Dickens, J. H. Moore, D. J. Neild, *J. Solid State Chem.* **1973**, *7*, 241–244.

[67] S. Wang, E. Iglesia, *J. Catal.* **2017**, *345*, 183–206.

[68] V. Pallassana, M. Neurock, *J. Catal.* **2002**, *209*, 289–305.

[69] J. E. Benson, H. W. Kohn, M. Boudart, *J. Catal.* **1966**, *5*, 307–313.

10.1002/cctc.201901302